Ultrafast Light-Induced Magnetization Dynamics of Ferromagnetic Semiconductors

J. Chovan, E. G. Kavousanaki, and I. E. Perakis

Institute of Electronic Structure and Laser, Foundation for Research and Technology-Hellas and Department of Physics, University of Crete, Heraklion, Greece

(Received 5 August 2005; published 6 February 2006)

We develop a theory of ultrafast light-induced magnetization dynamics in ferromagnetic semiconductors. We demonstrate magnetization control during femtosecond time scales via the interplay between nonlinear circularly polarized optical excitation, hole-spin damping, polarization dephasing, and Mn-hole-spin interactions. Our results show magnetization relaxation and precession for the duration of the optical pulse governed by the nonlinear optical polarizations and populations.

DOI: 10.1103/PhysRevLett.96.057402 PACS numbers: 78.47.+p, 72.25.Rb, 75.50.Pp, 78.20.Ls

With the discovery of III-Mn-V ferromagnetic semiconductors [1], one can envision a new class of multifunctional devices that combine information processing and storage on a single chip with low power consumption. One of the challenges facing such future devices concerns the speed of the basic processing unit. This is governed by the dynamics of the collective spin and its ability to respond quickly to time-dependent external fields. Ultrafast pump-probe magneto-optical spectroscopy has been used to study the magnetization dynamics triggered by femtosecond optical pulses in both metals [2,3] and ferromagnetic semiconductors [4–7]. Transient magnetic effects have been observed even in the initial nonthermal temporal regime, where the concept of carrier temperature is not meaningful [2,8].

In III-Mn-V semiconductors, the ferromagnetic order is induced by the interaction between the itinerant valence band hole spins and the localized Mn spins [9,10]. The magnetization is therefore sensitive to the itinerant carrier properties. In III–V semiconductors, these can be well controlled with ultrashort optical pulses [11]. The combined magnetic and optical properties of this system open new possibilities for manipulating the collective spin, e.g., by exciting spin-polarized carriers with circularly polarized optical pulses. The effects of such photoexcited spin on the ferromagnetic state can be studied by monitoring the change in the magnetization with time using ultrafast spectroscopy [2–7]. Light-induced magnetization and very fast Mn-spin rotation towards the direction of pulse propagation, perpendicular to the ground state magnetization, were reported in Ga(Mn)As ferromagnetic epilayers [7]. Kimel *et al.* [4] observed a photoinduced magnetization attributed to the photoexcited conduction electron spin. Kojima *et al.* [6] observed a picosecond rise in carrier temperature, followed by a slow rise in the spin temperature and a magnetization reduction over hundreds of ps. For very intense photoexcitation of In(Mn)As, Wang *et al.* [5] observed a fast (hundreds of fs) and a slow (hundreds of ps) demagnetization regime. Other possibilities for light-induced magnetic effects in nonmagnetic semiconductors were recently explored theoretically [12,13]. In doped semiconductors, a light-induced Kondo effect was predicted [12], while a light-induced paramagnetic-to-ferromagnetic phase transition was predicted in undoped semiconductors [13].

In this Letter, we develop a theory of the ultrafast nonlinear optical dynamics and light-induced hole and Mn-spin relaxation in ferromagnetic semiconductors. We predict an ultrafast light-induced precession and relaxation of the collective magnetization towards a direction determined by the nonlinear optical polarizations. The above spin dynamics results from the interplay between the nonlinear optical excitation, the interaction between the photoexcited hole and Mn spins, the strong hole-spin damping, and the optical polarization dephasing. The predicted dynamics is observable with ultrafast magneto-optical pump-probe spectroscopy.

We adopt the two-band sp-d model Hamiltonian [9,10] $H(t) = K_e + K_h + H_{\rm exch} + H_L(t)$, where K_h (K_e) is the kinetic energy of the valence band heavy holes (conduction band electrons) created by $\hat{h}^\dagger_{\mathbf{k}\sigma}$ ($\hat{e}^\dagger_{\mathbf{k}\sigma}$) with total angular momentum $J_z = \pm 3/2$ (spin $\sigma = \pm 1/2$) and dispersion $\varepsilon^v_{\mathbf{k}} = k^2/2m_h$ ($\varepsilon^c_{\mathbf{k}} = k^2/2m_e$) (we set $\hbar = 1$). Unlike in II–VI semiconductors, the Mn impurities provide a hole Fermi sea as well as randomly distributed $S = 5/2$ localized spins, $\mathbf{S}_j$, located at positions $\mathbf{R}_j$. The latter local moments interact strongly with the itinerant hole spins via the Kondo-like exchange interaction

$$H_{\rm exch} = \frac{J}{V} \sum_{j\mathbf{k}\mathbf{k}'\sigma\sigma'} (\mathbf{S}_j \cdot \sigma)_{\sigma\sigma'} e^{i(\mathbf{k}-\mathbf{k}')\cdot\mathbf{R}_j} \hat{h}^\dagger_{\mathbf{k}\sigma} \hat{h}_{\mathbf{k}'\sigma'}, \qquad (1)$$

where σ is the hole-spin operator and V is the volume. The coupling of right-circularly polarized optical fields is described in the rotating frame by [11]

$$H_L(t) = -d(t) \sum_{\mathbf{k}} \hat{e}^\dagger_{\mathbf{k}\downarrow} \hat{h}^\dagger_{-\mathbf{k}\uparrow} + \text{H.c.}, \qquad (2)$$

where $d(t) = \mu_{cv}\mathcal{E}(t)$ is the Rabi energy, μ_{cv} is the dipole transition matrix element, and $\mathcal{E}(t) \propto \exp[-t^2/\tau_p^2]$ is the optical pulse, with central frequency ω_p and duration τ_p. In the above Hamiltonian, the spin quantization z axis was taken parallel to the direction of optical pulse propagation,

which similar to Ref. [7] is chosen *perpendicular* to the ground state spin polarization.

The ground state, thermodynamic, and transport properties of III(Mn)V semiconductors are typically described by treating the spin interaction [Eq. (1)] within the mean field virtual crystal approximation [9,10,14–16]. This approximation neglects spatial correlations and assumes uniformly distributed classical Mn spins [9,10]. The holes experience an effective magnetic field proportional to the average Mn spin [9,10]. The valence states then split into two spin-polarized bands, separated by the magnetic exchange energy JcS, where c is the Mn concentration, and populated by the hole Fermi sea. The spins of the above bands point antiparallel and parallel to the Mn spin, which is taken here to define the x axis.

Here we describe the ultrafast nonlinear optical response of III(Mn)V semiconductors by solving the equations of motion for the density matrix. For right-circularly polarized light, spin-$\uparrow$ electron states are not populated, and we need to calculate only the interband optical polarizations $P_{\mathbf{k}\sigma} = \langle \hat{h}_{-\mathbf{k}\sigma}\hat{e}_{\mathbf{k}\downarrow}\rangle$, the carrier populations, the average Mn spin $\mathbf{S}$, and the hole spin $\mathbf{s}^h_{\mathbf{k}}$, with components $s^h_{\mathbf{k}z} = \sum_\sigma \sigma\langle \hat{h}^\dagger_{\mathbf{k}\sigma}\hat{h}_{\mathbf{k}\sigma}\rangle$ and $s^h_{\mathbf{k}+} = s^h_{\mathbf{k}x} + is^h_{\mathbf{k}y} = \langle \hat{h}^\dagger_{\mathbf{k}\uparrow}\hat{h}_{\mathbf{k}\downarrow}\rangle$. By factorizing all higher density matrices, we obtain a closed system of equations analogous to the semiconductor Bloch equations [11] with spin degrees of freedom. Because of the selection rules [Eq. (2)], right-circularly polarized light excites directly only the spin-$\uparrow$ hole polarization $P_\uparrow$:

$$\left(i\partial_t - \Omega_{\mathbf{k}} - \frac{JcS_z}{2}\right)P_{\mathbf{k}\uparrow} - \frac{JcS_-}{2}P_{\mathbf{k}\downarrow} = -d(t)[1 - \langle \hat{e}^\dagger_{\mathbf{k}\downarrow}\hat{e}_{\mathbf{k}\downarrow}\rangle - \langle \hat{h}^\dagger_{\mathbf{k}\uparrow}\hat{h}_{\mathbf{k}\uparrow}\rangle], \quad (3)$$

where $S_\pm(t) = S_x(t) \pm iS_y(t)$ and $\Omega_{\mathbf{k}} = \varepsilon^v_{\mathbf{k}} + \varepsilon^c_{\mathbf{k}} - \omega_p - i/T_2$, where T_2 is the polarization dephasing time. The right-hand side (r.h.s.) of the above equation describes the Pauli-blocking nonlinearity (phase space filling) [11]. This is determined by the equations of motion for the carrier populations, with initial condition the Fermi-Dirac distribution of the hole Fermi sea. Additional nonlinearities come from the light-induced changes in the Mn spin $\mathbf{S}(t)$ from its ground state configuration. These changes result in a time-dependent effective magnetic field $Jc\mathbf{S}(t)$ that depends nonlinearly on the optical excitation. This field gives a time-dependent e-h pair energy $\propto S_z(t)$, which renormalizes the spin-polarized hole bands, and a time-dependent coupling $\propto S_-(t)$ between $P_\uparrow$ and $P_\downarrow$:

$$\left(i\partial_t - \Omega_{\mathbf{k}} + \frac{JcS_z}{2}\right)P_{\mathbf{k}\downarrow} - \frac{JcS_+}{2}P_{\mathbf{k}\uparrow} = d(t)s^h_{\mathbf{k}+}. \quad (4)$$

$P_\downarrow$ is also generated by the hole-spin coherence, photoexcited or ground state, described by s^h_+ [r.h.s. of Eq. (4)]. In turn, the hole and Mn spins depend on the optical polarizations and precess due to the exchange interaction as described by the equations of motion:

$$\partial_t s^h_{\mathbf{k}} = Jc\mathbf{S}\times\mathbf{s}^h_{\mathbf{k}} + d(t)\mathbf{h}_{\mathbf{k}}, \qquad \partial_t\mathbf{S} = J\sum_{\mathbf{k}}\mathbf{s}^h_{\mathbf{k}}\times\mathbf{S}. \quad (5)$$

In the above equation, the photoexcited hole spin is determined by the nonlinear optical *polarizations* (and thus the interactions) as described by the vector

$$\mathbf{h}_{\mathbf{k}} = \mathrm{Im}(P_{\mathbf{k}\downarrow}, -iP_{\mathbf{k}\downarrow}, P_{\mathbf{k}\uparrow}). \quad (6)$$

During the femtosecond time scales of interest here, we neglected for simplicity the much slower precession and relaxation of the Mn spin due to magnetic anisotropy and Gilbert damping [14,15]. Unlike for calculations of the linear response, here we describe the nonlinear optical dynamics by solving numerically the above coupled equations without expanding in the optical field.

Most relaxation processes in III(Mn)V semiconductors occur during time scales longer than the pulse duration. A notable exception is hole-spin relaxation, which occurs within $\sim$10 fs due to the strong spin-orbit coupling in the valence band and the disorder-induced scattering between the different momentum states [15–17]. Such relaxation is typically described within the spin Bloch equations [14,17]. This is not adequate for our purposes since the hole-spin relaxation also dephases the optical polarizations and couples $P_\uparrow$ and $P_\downarrow$. Thus, the dephasing of both spin and optical polarizations must be treated on equal footing, including light-induced nonlinear corrections. Here we treat consistently all the above effects by using the Lindblad semigroup description of dissipative quantum dynamics [18]. Under the general assumptions of linear coupling between bath and system operators $L_{\mathbf{k}}$ and positivity and semigroup-type density matrix time evolution, the relaxation contribution is given by [18]

$$\partial_t\rho|_{\mathrm{rel}} = \sum_{\mathbf{k}\mathbf{k}'}\frac{\Gamma_{\mathbf{k}\mathbf{k}'}}{2}\langle 2L_{\mathbf{k}}\hat{\rho}L^\dagger_{\mathbf{k}'} - L^\dagger_{\mathbf{k}'}L_{\mathbf{k}}\hat{\rho} - \hat{\rho}L^\dagger_{\mathbf{k}'}L_{\mathbf{k}}\rangle. \quad (7)$$

The Lindblad operators $L_{\mathbf{k}} = \hat{h}^\dagger_{\mathbf{k}\Downarrow}\hat{h}_{\mathbf{k}\Uparrow}$, where $\hat{h}^\dagger_{\mathbf{k}\Uparrow}$ ($\hat{h}^\dagger_{\mathbf{k}\Downarrow}$) creates a hole with spin parallel (antiparallel) to the Mn spin, describe relaxation of the hole spin toward the direction opposite to $\mathbf{S}(t)$. In III(Mn)V semiconductors, this spin relaxation rate, $\Gamma_{\mathbf{k}\mathbf{k}'} = \delta_{\mathbf{k}\mathbf{k}'}\Gamma_s$, is mainly determined by the spin-orbit interaction [15,17]. Its magnitude, $1/\Gamma_s \sim$ 10 fs, is similar to the inverse scattering time between different momentum states [15,17] calculated in Ref. [16]. Important for our purposes is that $1/\Gamma_s$ is shorter than the hole-spin precession time. Additional contributions to Γ_s can arise from magnon-hole scattering [19], impurities, disorder, etc. The detailed equations, obtained from Eq. (7) by factorizing the higher density matrices, will be presented elsewhere. Here we note that the hole spin component perpendicular to $\mathbf{S}$ dephases with a rate Γ_s, while the spin component parallel to $\mathbf{S}$ relaxes with a rate $2\Gamma_s$ towards $-s_{\max} + s^2_{\max} - (\mathbf{s}^h_{\mathbf{k}})^2$, where $s_{\max}$, with $s_{\max} - s^2_{\max} = n^h_{\mathbf{k}}/2 - (n^h_{\mathbf{k}}/2)^2$, is the maximum hole spin for given number of holes $n^h_{\mathbf{k}} = \sum_\sigma\langle \hat{h}^\dagger_{\mathbf{k}\sigma}\hat{h}_{\mathbf{k}\sigma}\rangle$. Equation (7) also gives optical polarization dephasing and coupling

between $P_\uparrow$ and $P_\downarrow$ that depend on $\mathbf{S}(t)$, $\mathbf{s}^h(t)$, and the hole populations, to be discussed elsewhere. Scattering between the momentum states leads to an additional polarization dephasing described by $T_2 \sim 10$ fs $\sim 1/\Gamma_s$ [16].

Figure 1 shows the light-induced time evolution of the Mn spin for pulse duration $\tau_p = 250$ fs, $d = 60$ meV, detuning 10 meV below the threshold of interband absorption, exchange energy $JcS = 125$ meV, Fermi energy 100 meV, fraction of initial holes 0.33 of the Mn impurities, and $m_h/m_e = 7.15$. Γ_s, T_2, and T_1 in Fig. 1(c) are typical for III(Mn)V semiconductors [5,16]. The importance of hole-spin relaxation and polarization dephasing is clear by comparing Fig. 1(c) to the trajectories for longer $1/\Gamma_s$ and T_2 [Figs. 1(a) and 1(b)]. Hole-spin damping leads to a large Mn-spin z component, further enhanced by the short T_2. Note that the Mn spin rotates in a *clockwise* direction within the x-y plane perpendicular to the pulse propagation direction.

The spin dynamics of Fig. 1 comes from the Mn-spin precession around the time-dependent mean hole spin. The latter changes strongly with time, as determined by the nonlinear optical polarizations, the hole-spin relaxation, and the precession around $\mathbf{S}$ [Eq. (5)]. The hole spin follows overall the Mn-spin trajectory, with the exception of a component perpendicular to $\mathbf{S}$ that triggers the Mn-spin dynamics. The light-induced deviations from the equilibrium spin configurations occur *within the pulse duration* and increase with its duration and intensity.

At first glance, the clockwise Mn-spin rotation is surprising, given that, due to the selection rules Eq. (2), right-circularly polarized light creates spin-up holes. These should lead to *counterclockwise* rotation [Eq. (5)]. However, our numerical results show that the photoexcited hole-spin z component is negative due to the exchange interaction. This is a consequence of the photoexcitation of $\mathbf{s}^h$ by the nonlinear optical polarizations rather than the optical field directly [see Eq. (5)]. Also striking is the strong effect of the hole-spin relaxation on the Mn-spin trajectory. It leads to the development, within the pulse duration, of a large component S_z in the direction of optical pulse propagation. This component develops in the absence of Mn-spin damping in Eq. (5). A very fast Mn-spin tilt toward the z direction was observed experimentally [7], however, for weaker photoexcitation. The above spin dynamics is significant for Rabi energies larger than a few tens of meVs. This corresponds to stronger photoexcitation than in Ref. [4] but not as strong as in Ref. [5], where hole heating [2] becomes pronounced.

To interpret our numerical results, we consider the stationary (adiabatic following) limit relevant to our system. In this limit, the hole-spin precesses and/or relaxes much faster than the pulse duration and period of Mn-spin precession. It thus adjusts to the instantaneous $d(t)$ and $\mathbf{S}(t)$ values. Neglecting the component of $\partial_t \mathbf{s}^h$ perpendicular to $\mathbf{S}$, we can then eliminate the hole spin from Eq. (5) and obtain after some algebra and noting that $\mathbf{S} \cdot \partial_t \mathbf{S} = 0$,

$$\partial_t \mathbf{S} = \frac{Jd(t)}{(JcS)^2 + \Gamma_s^2}[\Gamma_s \mathbf{h} \times \mathbf{S} - JcS \times (\mathbf{S} \times \mathbf{h})], \quad (8)$$

where $\mathbf{h}(t) = \sum_{\mathbf{k}} h_{\mathbf{k}}(t)$ is an effective magnetic field determined by the nonlinear optical polarizations [Eq. (6)]. Equation (8) demonstrates light-induced precession around $\mathbf{h}(t)$ and Gilbert dampinglike relaxation of $\mathbf{S}$ toward $\mathbf{h}(t)$. These effects should be contrasted to the static effects governed by the magnetic anisotropy [14,15].

The light-induced effective magnetic field $\mathbf{h}(t)$ [Eq. (6)] that governs the Mn-spin dynamics has z component determined by the dissipative part of the nonlinear optical polarization, $\mathrm{Im}P_\uparrow$, and in-plane components determined by $P_\downarrow$. Its time dependence is shown in Fig. 2. The exchange interaction plays an important role in determining $\mathbf{h}(t)$. To see this, let us consider $J = 0$. In this case, $P_\downarrow = 0$. $\mathbf{h}$ then points along the z axis and its magnitude is determined by the dephasing of $P_\uparrow$. For $T_2 < \tau_p$, $\mathbf{h}$ is proportional to the optical pump rate. The Mn spin would then relax to the z axis. However, the exchange interaction and

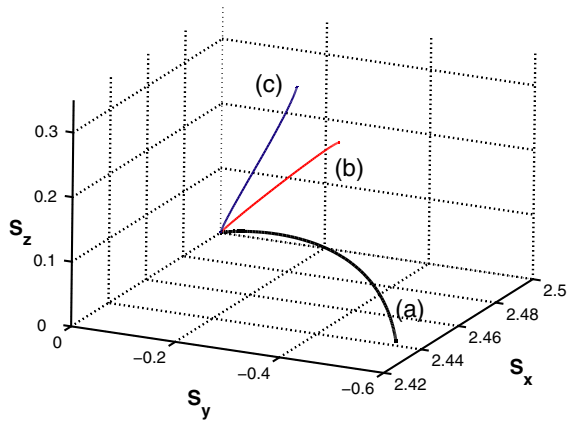

FIG. 1 (color online). Dependence of Mn-spin trajectory on the relaxation: (a) $T_2 = 2T_1 = 330$ fs, $\Gamma_s = 0$ (coherent limit); (b) $T_2 = 2T_1 = 330$ fs, $1/\Gamma_s = 10.5$ fs; (c) $T_1 = 165$ fs, $T_2 = 1/\Gamma_s = 10.5$ fs.

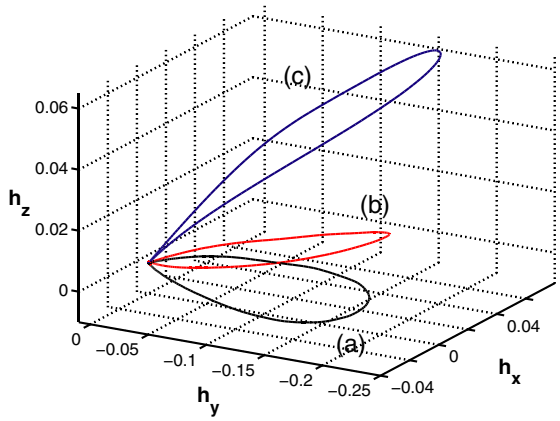

FIG. 2 (color online). Trajectories of the light-induced field $\mathbf{h}$ (units of $d(0)/2E_F$) for the three relaxation regimes of Fig. 1.

spin relaxation drastically affect the optical polarizations and thus $\mathbf{h}(t)$. For example, by coupling the hole-spin-$\uparrow$ and spin-$\downarrow$ states, they lead to a large $P_\downarrow$ and thus a large x-y plane component of the effective magnetic field $\mathbf{h}$. This is demonstrated in Fig. 2, which shows $\mathbf{h}(t)$ for different values of the relaxation rates. In fact, for sufficiently long T_2 and detunings close to or below the interband absorption threshold, $\mathrm{Re}P_\downarrow$ exceeds $\mathrm{Im}P_\uparrow$. In this case, the light-induced magnetic field $\mathbf{h}$ points mostly along the x-y plane, in a direction almost perpendicular to the ground state magnetization (x axis) [see Fig. 2(a)]. For $\Gamma_s = 0$, the second term on the r.h.s. of Eq. (8) then leads to Mn-spin relaxation mostly within the x-y plane. With increasing Γ_s, the first term leads to an additional precession out of the x-y plane, consistent with the numerical results of Fig. 1. The polarization dephasing, due to the hole-spin damping as well as the disorder and other contributions, enhances the relative magnitude of $\mathrm{Im}\mathbf{P}_\uparrow$ and thus h_z [see Figs. 2(b) and 2(c)]. As a result of h_z, $\mathbf{S}$ develops an additional z component as it relaxes toward $\mathbf{h}$. One should note that the r.h.s. of Eq. (8) vanishes after the optical pulse is gone and thus the light-induced Mn-spin relaxation and precession occurs only during the pulse. Furthermore, the optical polarizations, and therefore $\mathbf{h}(t)$, depend on the spins. Thus the Mn-spin dynamics leads to an additional time dependence of $\mathbf{h}(t)$ and to corresponding nonlinearities. This can be seen in Fig. 2, where the trajectories of $\mathbf{h}(t)$ have a looplike shape. Finally, the phase space filling optical nonlinearity affects the time dependence of $\mathbf{h}(t)$ [Eq. (6)], and thus the Mn-spin relaxation Eq. (8).

To gain insight into the effects of the nonlinear optical excitation and exchange interaction on the hole-spin dynamics, we solved analytically the polarization equations of motion [Eqs. (3) and (4)] for $T_2 < \tau_p$ in the stationary limit (to be discussed elsewhere). For example, we obtained for the x-y spin components ($\Gamma_s = 0$)

$$\partial_t s^h_{\mathbf{k}+} = J\left[1 + \frac{d^2(t)/2}{\Omega^2_{\mathbf{k}} - (JcS/2)^2}\right]\mathbf{S} \times \mathbf{s}^h_{\mathbf{k}}|_+ + \frac{id^2(t)\Omega_{\mathbf{k}}}{\Omega^2_{\mathbf{k}} - (JcS/2)^2}\left[s^h_{\mathbf{k}+} + \frac{J(1 - n_{\mathbf{k}}/2)}{2\Omega_{\mathbf{k}}} S_+\right], \tag{9}$$

where $n_{\mathbf{k}} = \sum_\sigma \langle \hat{h}^\dagger_{\mathbf{k}\sigma} \hat{h}_{\mathbf{k}\sigma} \rangle$. The first term on the r.h.s. describes hole-spin precession around $\mathbf{S}(t)$ triggered by a time-dependent effective exchange interaction. The second term describes a light-induced x-y plane rotation of the hole spin, even for $S_z = 0$, while its dissipative part describes a light-induced hole-spin relaxation. Finally, we note that, for very strong photoexcitation [5] and/or detunings well above the absorption edge, the heating of the hole Fermi sea can become significant. Similar to metals [2], such hot hole effects can be treated by introducing a time-dependent temperature to our equations.

In conclusion, we presented a theory of ultrafast nonlinear optical and spin dynamics in III(Mn)V ferromagnetic semiconductors. We demonstrated a light-induced Mn-spin precession and relaxation, which can lead to a magnetization tilt of several tens of degrees. We showed that the latter is determined by the nonlinear optical polarizations and depends critically on the exchange interactions, dephasing, and hole-spin relaxation. The nonlinear light-induced magnetic effects discussed here occur during the optical pulse and can be observed with ultrafast pump-probe magneto-optical spectroscopy. The role of the fluctuations, the carrier-magnon correlations [19], the disorder, and the valence band structure on the ultrafast dynamics should be considered in the future.

This work was supported by the EU Research Training Network HYTEC (HPRN-CT-2002-00315).

[1] H. Ohno, Science **281**, 951 (1998).
[2] M. Vomir *et al.*, Phys. Rev. Lett. **94**, 237601 (2005); L. Guidoni, E. Beaurepaire, and J.-Y. Bigot, Phys. Rev. Lett. **89**, 017401 (2002), and references therein.
[3] B. Koopmans *et al.*, Phys. Rev. Lett. **85**, 844 (2000).
[4] A. V. Kimel *et al.*, Phys. Rev. Lett. **92**, 237203 (2004).
[5] J. Wang *et al.*, Phys. Rev. Lett. **95**, 167401 (2005).
[6] E. Kojima *et al.*, Phys. Rev. B **68**, 193203 (2003).
[7] A. Oiwa *et al.*, Phys. Rev. Lett. **88**, 137202 (2002); Y. Mitsumori *et al.*, Phys. Rev. B **69**, 033203 (2004).
[8] R. Gomez-Abal *et al.*, Phys. Rev. Lett. **92**, 227402 (2004); G. P. Zhang and W. Hübner, Phys. Rev. Lett. **85**, 3025 (2000).
[9] T. Dietl *et al.*, Science **287**, 1019 (2000); T. Jungwirth *et al.*, Phys. Rev. B **72**, 165204 (2005).
[10] See, e.g., J. König *et al.*, in *Electronic Structure and Magnetism of Complex Materials*, edited by J. Singh and D. A. Papaconstantopoulos (Springer-Verlag, Berlin, 2003).
[11] See, e.g., W. Schäfer and M. Wegener, *Semiconductor Optics and Transport Phenomena* (Springer-Verlag, Berlin, 2002); N. Linder and L. J. Sham, Physica (Amsterdam) **2E**, 412 (1998).
[12] T. V. Shahbazyan, I. E. Perakis, and M. E. Raikh, Phys. Rev. Lett. **84**, 5896 (2000).
[13] J. Fernández-Rossier *et al.*, Phys. Rev. Lett. **93**, 127201 (2004).
[14] Y. Tserkovnyak, G. A. Fiete, and B. I. Halperin, Appl. Phys. Lett. **84**, 5234 (2004).
[15] A. H. Mitchell, Phys. Rev. **105**, 1439 (1957); J. Sinova *et al.*, Phys. Rev. B **69**, 085209 (2004); J. Fernández-Rossier *et al.*, cond-mat/0304492.
[16] T. Jungwirth *et al.*, Appl. Phys. Lett. **81**, 4029 (2002); J. Sinova *et al.*, Int. J. Mod. Phys. B **18**, 1083 (2004).
[17] I. Zutic, J. Fabian, and S. Das Sarma, Rev. Mod. Phys. **76**, 323 (2004).
[18] G. Lindblad, Commun. Math. Phys. **48**, 119 (1976); R. Kosloff and S. A. Rice, J. Chem. Phys. **72**, 4591 (1980).
[19] M. D. Kapetanakis, A. Manousaki, and I. E. Perakis, cond-mat/0601025; V. Yu. Irkhin and M. I. Katsnelson, Eur. Phys. J. B **19**, 401 (2001), and references therein.